ISSN 0006-2979, Biochemistry (Moscow), 2026, Vol. 91, No. 10, pp. 1971-1978 © Pleiades Publishing, Ltd., 2026.

Features of Intracellular Events in Respiratory Burst and Regulated Neutrophil Death Caused by Phorbol-12-Myristate-13-Acetate (PMA)

Mikhail A. Panteleev[1,2,3,a]*, Elena O. Artemenko[1,2], Ekaterina A. Adamanskaya[1,2], Quhuan Li[4], Aleksey V. Sokolov[5], and Anastasia N. Sveshnikova[1,2,3]

[1]*Center for Theoretical Problems of Physicochemical Pharmacology, Russian Academy of Sciences, 109029 Moscow, Russia*

[2]*Dmitry Rogachev National Medical Research Center of Pediatric Hematology, Oncology and Immunology, Ministry of Health of the Russian Federation, 117198 Moscow, Russia*

[3]*Faculty of Physics, Lomonosov Moscow State University, 119991 Moscow, Russia*

[4]*South China University of Technology, 510640 Guangzhou, China*

[5]*Institute of Experimental Medicine, 197022 Saint Petersburg, Russia*

[a]*e-mail: mapanteleev@yandex.ru*

Received July 25, 2026
Revised October 7, 2026
Accepted October 9, 2026

Abstract—Respiratory (oxidative) burst of neutrophils is explosive formation of reactive oxygen species controlled by a complex intracellular signaling network. If activation of the respiratory burst is sufficiently prolonged and intense, it could initiate regulated cell death through various mechanisms, the best known of which is NETosis, a specific form of lytic regulated cell death involving release of extracellular DNA networks. We investigated dynamics, concentration dependence, and activation parameters of the respiratory burst and regulated death of human neutrophils upon stimulation of protein kinase C with the diacylglycerol mimetic, phorbol 12-myristate 13-acetate (PMA), using flow cytometry and fluorescence microscopy. When isolated neutrophils were activated with PMA, the fastest and most sensitive response was granule secretion, assessed by CD63 expression using flow cytometry. Reactive oxygen species (ROS) generation followed next in the temporal and concentration hierarchy of responses. Lytic death of neutrophils observed by flow cytometry followed the ROS generation and occurred at the same activator concentrations. Yet, as the PMA concentration increased, the number of neutrophils recorded by the cytometer decreased substantially, indicating complete cell destruction. To determine the extent of this destruction, we examined response of the neutrophils in the leukocyte-rich blood plasma by fluorescence microscopy in a flow chamber, where the dynamics of the process was considerably slower. Pronounced cell lysis occurred in response to PMA activation via both the NETosis and necrosis pathways. ROS generation became concentrated in the individual neutrophil vacuoles within several tens of minutes after activation. Overall, in response to activation, neutrophils display a classic sequence of signaling events, which could culminate in a respiratory burst accompanying phagocytosis, necrosis, NETosis, or secondary necrosis.

DOI: 10.1134/S0006297926602546

Keywords: neutrophils, protein kinase C, necrosis, neutrophil extracellular DNA traps, NETosis, reactive oxygen species

INTRODUCTION

Neutrophils are the most numerous leukocyte subtype in blood, responsible for phagocytosing pathogenic microorganisms and decay of the products of destruction of the body's own cells. The key physiological response of a neutrophil to stimulation (uptake of a pathogen or exposure to activating substances secreted by other cells) is respiratory,

* To whom correspondence should be addressed.

or oxidative, burst [1]. This response is driven mainly by the generation of reactive oxygen species (ROS) by the NADPH oxidase 2 (NOX) enzyme in the neutrophil phagosome or vacuoles, with the aim of eliminating bacteria [2]. Depending on the type of stimulation, mitochondrial ROS could also contribute to the respiratory burst [3]. ROS additionally play a signaling role in this process, regulating the respiratory burst [4] and subsequently driving a subset of neutrophils toward the specialized form of regulated cell death, release of the neutrophil extracellular traps (NETs), or NETosis [5].

NETosis is a lytic variant of cell death in which the cell expels DNA strands possessing antimicrobial activity. It is a rather ancient mechanism of immune defense, known even in invertebrates and social amoebae [6], and is not confined to neutrophils. Beyond the immune defense, it plays important roles in pathophysiology of a wide range of disorders, including sepsis, coronavirus infection, deep vein thrombosis, and many others [7-9].

The key intracellular signaling enzyme mediating the respiratory burst is protein kinase C (PKC) [10]. For this reason and given technical difficulty of physiologically activating the respiratory burst and NETosis, stimulation with the protein kinase C activator phorbol 12-myristate 13-acetate (PMA), a mimetic of diacylglycerol, is a widespread experimental model [11]. Nevertheless, overall picture of the respiratory burst and NETosis in the context of possible scenarios of the regulated neutrophil death [12] remains poorly understood. In this work, we quantitatively characterized the neutrophil response to PMA using flow cytometry and fluorescence microscopy, in order to establish, within two complementary experimental settings, the following key parameters: time course of the main events with corresponding characteristic times; hierarchy of various neutrophil responses as a function of the degree of activation, together with the corresponding critical activator concentrations; spatial localization of ROS; proportions of the different death scenarios during activation; and importance of immobilization and environment for studying neutrophil responses.

MATERIALS AND METHODS

Reagents. The following fluorescent dyes were used: Hoechst 33342 (Sigma-Aldrich Co., USA); Sytox Green (Thermo Fisher Scientific, USA); annexin V conjugated with the fluorophore AF647 (Lumiprobe, Russia); anti-CD63-FITC antibody (Sony Biotechnology, USA); a reactive oxygen species dye 2′,7′-dichlorodihydrofluorescein diacetate (H2DCFDA, Thermo Fisher Scientific, USA); and an extracellular DNA dye 7-aminoactinomycin D (7-AAD, Lumiprobe, Russia). We also used Ficoll with densities of 1.119 and 1.077 g/cm^3 (PanEco, Russia), Percoll with density of 1.135 g/cm^3 (GE Healthcare, USA), PMA (phorbol 12-myristate 13-acetate; Sigma-Aldrich, USA), and poly-L-lysine (Sigma-Aldrich Co., USA). Experiments were performed in a modified Tyrode buffer (150 mM NaCl, 2.7 mM KCl, 1 mM $MgCl_2$, 0.4 mM NaH_2PO_4, 0.4 mM $NaHCO_3$, 2.5 mM $CaCl_2$, 20 mM HEPES, 5 mM glucose, 0.5% bovine serum albumin, pH 7.34); the reagents for this buffer were purchased from Sigma-Aldrich, USA.

Blood collection for preparation of leukocyte-rich plasma. Venous blood from healthy adult volunteers was collected into tubes coated with lithium-heparin as anticoagulant (MiniMed, Russia). The study was carried out in accordance with the Declaration of Helsinki and approved by the Ethics Committee of the Center for Theoretical Problems of Physicochemical Pharmacology, Russian Academy of Sciences (protocol no. 1 of January 12, 2018). Blood was processed within 3 h of collection. Leukocyte-rich plasma (LRP) was prepared by allowing the blood to settle for 45 min at 37°C. The LRP was next transferred to a separate tube, stained with Hoechst 33342 (1 : 1000), Sytox Green (1 : 10,000), and annexin V-AF647 (1 : 1000), and loaded into a microfluidic chamber. Partial activation of neutrophils cannot be excluded with the LRP preparation protocols used. All results were nevertheless processed identically, permitting relative comparisons between the “control” and “activation” experiments.

Isolation of neutrophils. Blood was collected into 10-ml EDTA-coated anticoagulant tubes (BD Vacutainer, USA). Blood samples were centrifuged at 100*g* for 8 min, after which the platelet-rich plasma upper layer was removed and replaced with an equal volume of PBS (10 mM sodium phosphate, 137 mM sodium chloride, 2.7 mM potassium chloride, pH 7.4). For neutrophil isolation on a Ficoll gradient, 3 ml of Ficoll with density of 1.119 g/cm^3 (PanEco) was layered into a 15-ml tube, and 3 ml of Ficoll with density of 1.077 g/cm^3 (PanEco) was carefully layered on top. Next 3 ml of a platelet-depleted blood was layered on top. The tube was centrifuged at 700*g* until all erythrocytes had visually settled to the bottom; centrifugation time was between 60 and 120 min depending on the donor. A ring at the interface between the two Ficoll phases, containing neutrophils, was carefully collected, and the cells were washed by adding a ten-fold excess of a Tyrode buffer (20 mM HEPES, 150 mM NaCl, 2.7 mM KCl, 1 mM $MgCl_2$, 0.4 mM NaH_2PO_4, 5 mM glucose, 0.5% bovine serum albumin, pH 7.4) and centrifuging at 200*g* for 10 min. The supernatant was removed, and the cells were resuspended in 1 ml of a Tyrode buffer, pH 7.4. For neutrophil isolation on a Percoll gradient,

the cells resuspended in 1 ml of a Tyrode buffer (pH 7.4) were layered onto a Percoll gradient of 62% and 75% (1 ml each). The tube was next centrifuged at 200*g* for 20 min. A fraction at the interface between the two Percoll solutions was collected, diluted ten-fold with a Tyrode buffer (pH 7.4), and centrifuged at 200*g* for 10 min. The supernatant was removed, and the cell pellet was resuspended in 400 µl of a Tyrode buffer, pH 7.4. Smears of isolated neutrophils stained with a Romanowsky–Giemsa stain were analyzed by microscopy. The results indicated approximately 90% neutrophil purity based on analysis of three donors.

Activation, staining, and flow cytometry. Isolated neutrophils with the cell count of 5000 cells/µl were incubated with 0.5 µM H_2DCFDA for 15 min at 37°C in a Tyrode buffer (pH 7.4), next diluted five-fold with the same buffer, pelleted by centrifugation at 200*g* for 10 min, and resuspended in a Tyrode buffer, pH 7.4. Neutrophils at 5000 cells/µl were activated by adding PMA up to 1.6 to 100 nM in a Tyrode buffer (pH 7.4) containing 2.5 mM calcium chloride followed by incubation for the indicated times at 37°C. Activated neutrophils were stained for 5 min at 37°C with CD63-FITC (final antibody concentration of 1%) and 7-AAD (final dye concentration of 5 µg/ml). The stained samples were next diluted with a Tyrode buffer (pH 7.4) supplemented with 2.5 mM calcium chloride and immediately analyzed using a Novocyte flow cytometer (ACEA Biosciences, USA); 50-µl samples were analyzed until several thousand events were collected within the neutrophil gate. Absence of mononuclear cells was verified using an FSC-versus-SSC gate (data not shown).

Microfluidic chambers. NETosis induced by PMA was observed in a parallel-plate flow chamber coated with poly-L-lysine (0.1%). LRP and working solutions were passed through the chamber by spontaneous gravity-driven flow without direct mechanical action. After entering the chamber, the blood was incubated for 10 min to allow cell adhesion to the substrate. Working concentration (100 nM) of PMA was prepared in a modified Tyrode buffer supplemented with Sytox Green (1 : 10000) and annexin V-AF647 (1 : 1000). PMA solution was introduced into the chamber and left there until the end of the experiment. NETosis observation system in the microfluidic setup thus operated in a stasis mode without medium renewal; this design was chosen to minimize mechanical impact on the cells and to exclude external influences from flow changes or the human factor. Observations were carried out with a Nikon Ti2 AX confocal microscope for 13 h. The resulting video sequences were analyzed and processed with the dedicated software NIS-Elements Viewer (version 5.22.00) and ImageJ (version 1.54f).

RESULTS

Dynamics and concentration dependence of the responses of isolated neutrophil in suspension to PMA. Isolated neutrophils were stimulated with 1.6-100 nM PMA, stained, and analyzed on a flow cytometer (Figs. 1 and 2). Granule secretion in the isolated neutrophils, assessed by CD63 expression, was the most sensitive response (Fig. 2a), reaching its half-maximal value at EC50 ~3 nM PMA. ROS generation, evaluated based on the H_2DCFDA fluorescence (Fig. 1, c and d), increased bilinearly (Fig. 2b) and required higher activator concentrations, with EC50 ~10 nM. The fraction of membrane-damaged/7-AAD-positive cells (Fig. 2c) – events scored as H_2DCFDA-negative and 7-AAD-positive (Fig. 1, g and h) – changed in roughly the same way. Notably, total number of the events detected by the cytometer dropped markedly with the increasing activation level (Fig. 2d), pointing to possible limitations of flow cytometry in this suspension setup, likely associated with rapid cell lysis.

Time dependence of the granule secretion, ROS generation, and formation of the membrane-damaged/7-AAD-positive population in response to PMA followed the same hierarchy: granule secretion (Fig. 2e) was the fastest (t_{lag} < 5 min), which was followed by ROS generation (Fig. 2f). Gradual decline of ROS generation over time in the control could be related both to the cell activation during isolation and to gradual leakage of the indicator from the cells. Formation of the membrane-damaged/7-AAD-positive cells was the slowest of the responses (Fig. 2g): the number of such cells grew linearly reaching maximum at 60 min. Cell lysis occurred rapidly, detected as decrease in the number of recorded events (Fig. 2h) within the very first minutes after activation.

Dynamics of NETosis and necrosis in neutrophils in LRP. To visualize the neutrophil activation process and analyze environmental effects, experiments were performed in a microfluidic chamber with leukocyte-rich blood plasma (Figs. 3 and 4). In contrast to flow cytometry, characteristic time of the neutrophil extracellular trap formation was on the order of hours (Fig. 3). By hour 5, most neutrophils had stopped moving and merely oscillated around their final position. By hour 7, the neutrophil nucleus began to deform, and by hour 8 the first signs of chromatin decondensation (loose structure) appeared. The next stage of NETosis – rupture of the nuclear membrane and release of the nuclear contents into the cytoplasm – occurred around the hour 9. Two hours later, the plasma membrane ruptured and the DNA was released from the cell. Even an hour after that, the networks continued to spread.

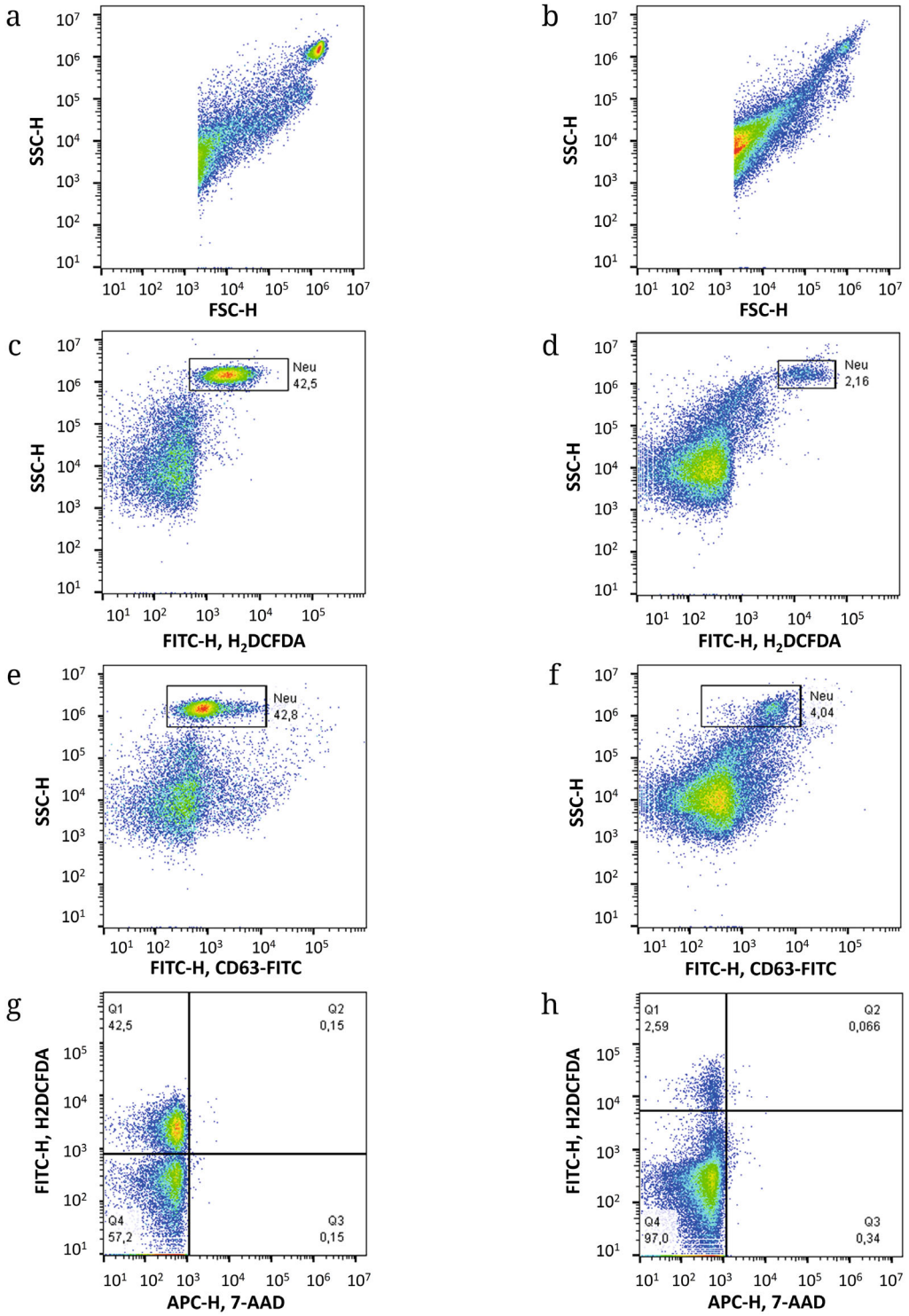

Fig. 1. Typical dot plots of non-activated and activated neutrophils. a) Non-activated neutrophils, 60 min, forward and side light scatter. b) Neutrophils activated with 100 nM PMA, 60 min, forward and side light scatter. c) Non-activated neutrophils, 60 min, side light scatter and fluorescence of the ROS dye H_2DCFDA; neutrophil region is outlined. d) Neutrophils activated with 100 nM PMA, 60 min, side light scatter and fluorescence of the ROS dye H_2DCFDA; neutrophil region is outlined. e) Non-activated neutrophils, 60 min, side light scatter and fluorescence of anti-CD63 antibodies (FITC-H); neutrophil region is outlined. f) Neutrophils activated with 100 nM PMA, 60 min, side light scatter and fluorescence of anti-CD63 antibodies (FITC-H); neutrophil region is outlined. g) Non-activated neutrophils, 60 min, fluorescence of the ROS dye H_2DCFDA (FITC-H) and the plasma membrane integrity dye 7-AAD (APC-H); all events are shown. Q1 – live cells with intact membrane; Q3 – dead cells with damaged membrane. h) Neutrophils activated with 100 nM PMA, 60 min, fluorescence of the ROS dye H_2DCFDA (FITC-H) and the membrane integrity dye 7-AAD (APC-H); Q1 – live cells with intact membrane; Q3 – dead cells with damaged membrane.

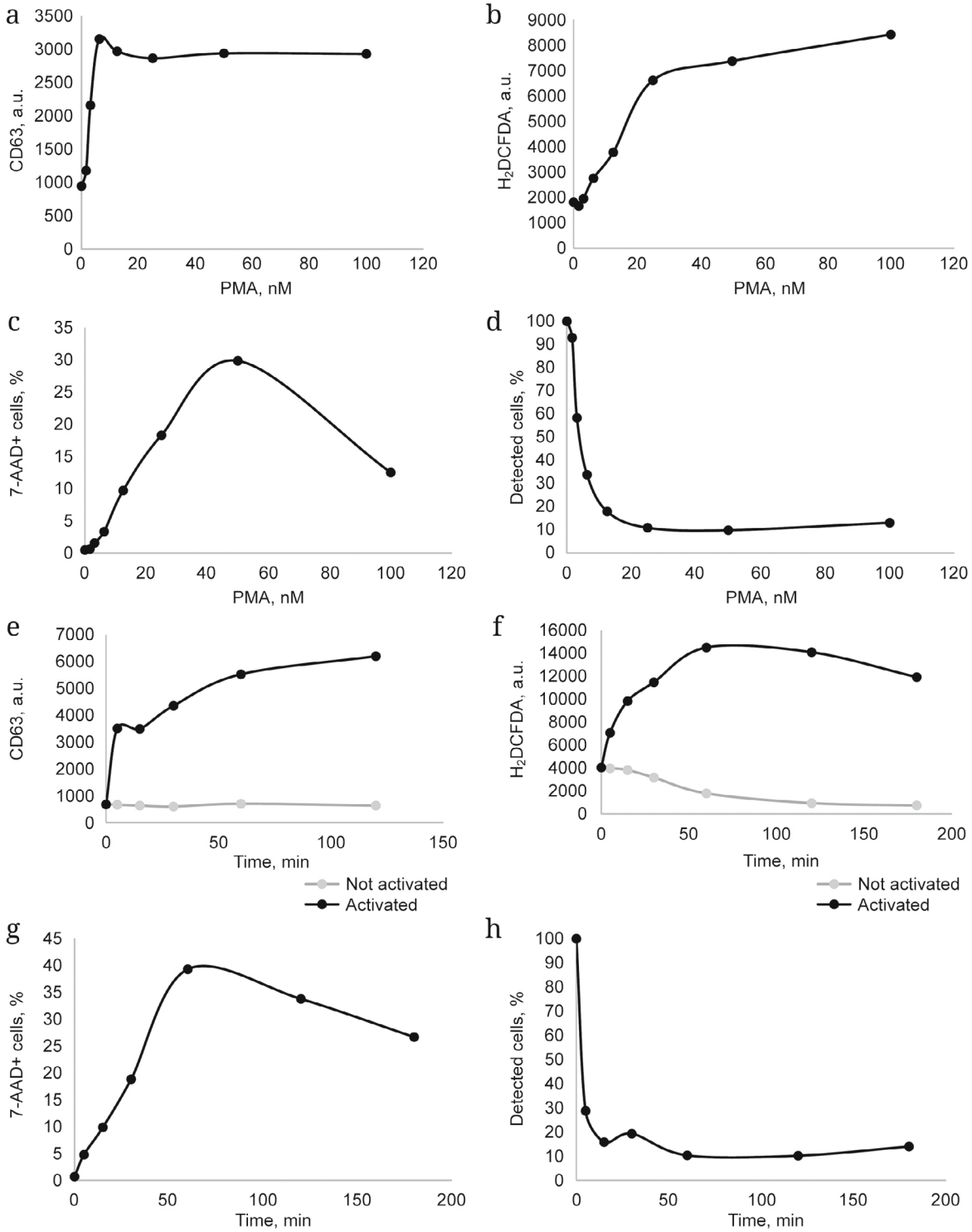

Fig. 2. Kinetics and dose-dependencies of neutrophil activation by PMA. Results of a typical experiment (n = 4) are shown. a) Granule release, detected by monitoring fluorescence of the cell-bound CD63-FITC, as a function of PMA concentration; data are shown for an activation time of 60 min. b) Detection of ROS generation in neutrophils by monitoring fluorescence of the H_2DCFDA dye as a function of PMA concentration; data are shown for an activation time of 60 min. c) Detection of membrane-damaged cells based on 7-AAD binding as function of PMA concentration; data are shown relative to the cells detectable at the given moment for an activation time of 60 min. d) Percentage of detectable cells as function of PMA concentration for activation time of 60 min. e) Kinetics of granule release upon neutrophil activation with 100 nM PMA, detected based on the CD63-FITC binding. f) Kinetics of ROS generation in neutrophils activated with 100 nM PMA, detected based on the H_2DCFDA fluorescence. g) Kinetics of neutrophil death upon activation with 100 nM PMA, detected based on the 7-AAD binding; percentage of neutrophils detectable at the given moment is shown. h) Percentage of detectable neutrophils relative to the initial number over time during activation with 100 nM PMA.

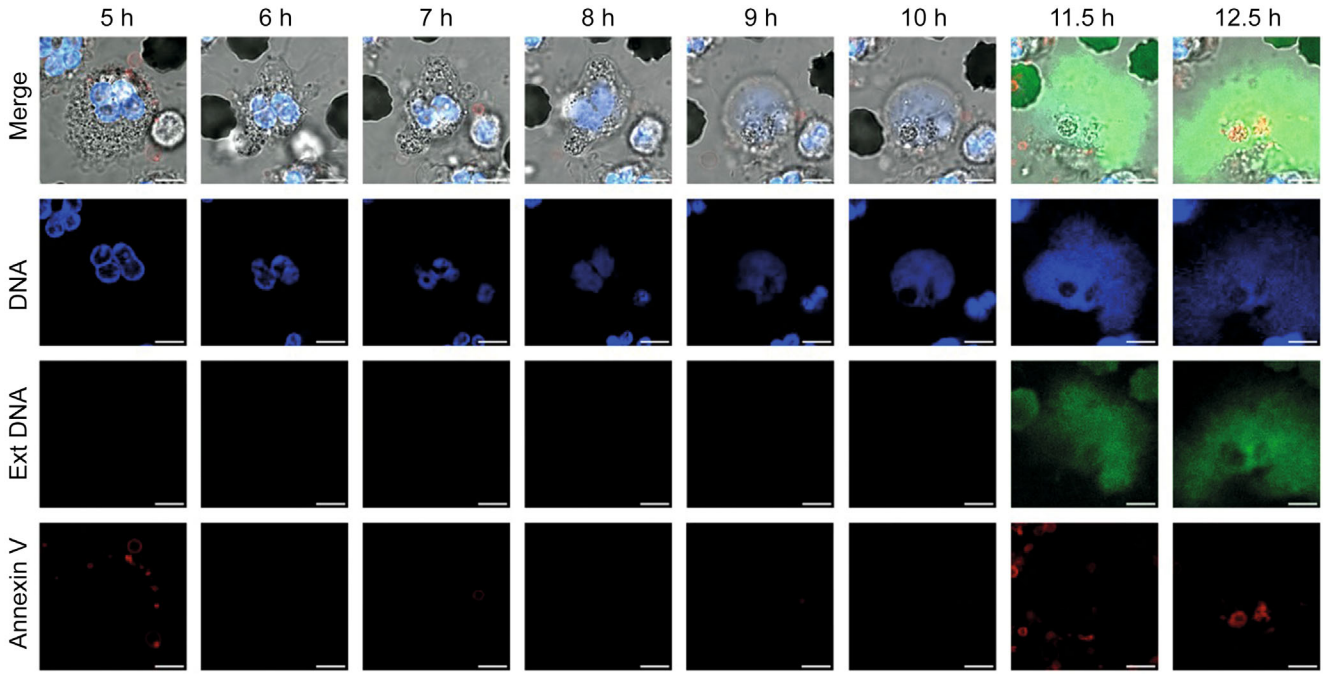

Fig. 3. Process of suicidal NETosis. The series of images shows stages of a typical transformation of a representative neutrophil in the microfluidic chamber in the presence of the activator (100 nM PMA). Blue – Hoechst 33342; green – Sytox Green; red – annexin V-AF647. Scale bar: 5 μm.

A detailed set of typical scenarios is shown in Fig. 4. Over time, the number of intact neutrophils (blue line in Fig. 4a) decreased. An intact neutrophil is characterized by a segmented nucleus, condensed chromatin, rounded shape, and presence of pseudopodia (Fig. 4b). Pre-NETosis was shown based on the assessment of the number of neutrophils with chromatin already decondensed and nuclear membrane ruptured while the plasma membrane was still preserved. The first "pre-NETotic" neutrophils (with decondensed nucleus but intact plasma membrane) appeared as early as 30 min after addition of the stimulator (the purple line). Cell necrosis (blistering of the cytoplasm, membrane rupture without DNA release) was manifested one hour after the start of the experiment (red line). Proper NETosis was defined by the release of decondensed DNA beyond the plasma membrane into the extracellular space. The first NETotic event was recorded at the hour 2, and massive transition of the neutrophils into NETosis was observed from the hour 5 (green line). By hour 13, the number of intact cells was 6, and the number of NETotic events was 74. At the beginning of the experiment (Fig. 4c), most cells had an undeformed nucleus, and only a few cells bound annexin V. By the end of the experiment, most neutrophils had undergone NETosis, while a fraction of the cells (including other leukocytes) had undergone necrosis. Early in the experiment, the cell moved by chemotaxis (Fig. 4d); it then stopped and began oscillating around its final position. From there, the cell could either undergo NETosis or undergo necrosis. In the control experiments without PMA, the first signs of NETosis appeared only 9 h after the start of the experiment, and active process took place after 14 h (data not shown).

DISCUSSION

Dynamics and patterns of PMA-induced neutrophil death observed in this work point to several technical and fundamental features of the process. The overall phenomenon seen by flow cytometry is close to the previous descriptions of NETosis [5, 13, 14]. In this work, a single experimental design allows quantitative description of the hierarchy of the activation responses depending on time and concentration: granule release, ROS generation, and neutrophil death follow one another. Moreover, monitoring of the event counts shows that flow cytometric methods could miss more than half of the cells under these conditions. Absence of large events (possible aggregates) in the cytometry data, combined with the dynamic fluorescence microscopy, indicates that PMA stimulation drives cells into both NETosis and necrosis and that a substantial fraction of cells lyse completely, which requires corrections to the quantitative estimates.

The characteristic response times of neutrophils in plasma are markedly longer than those for washed

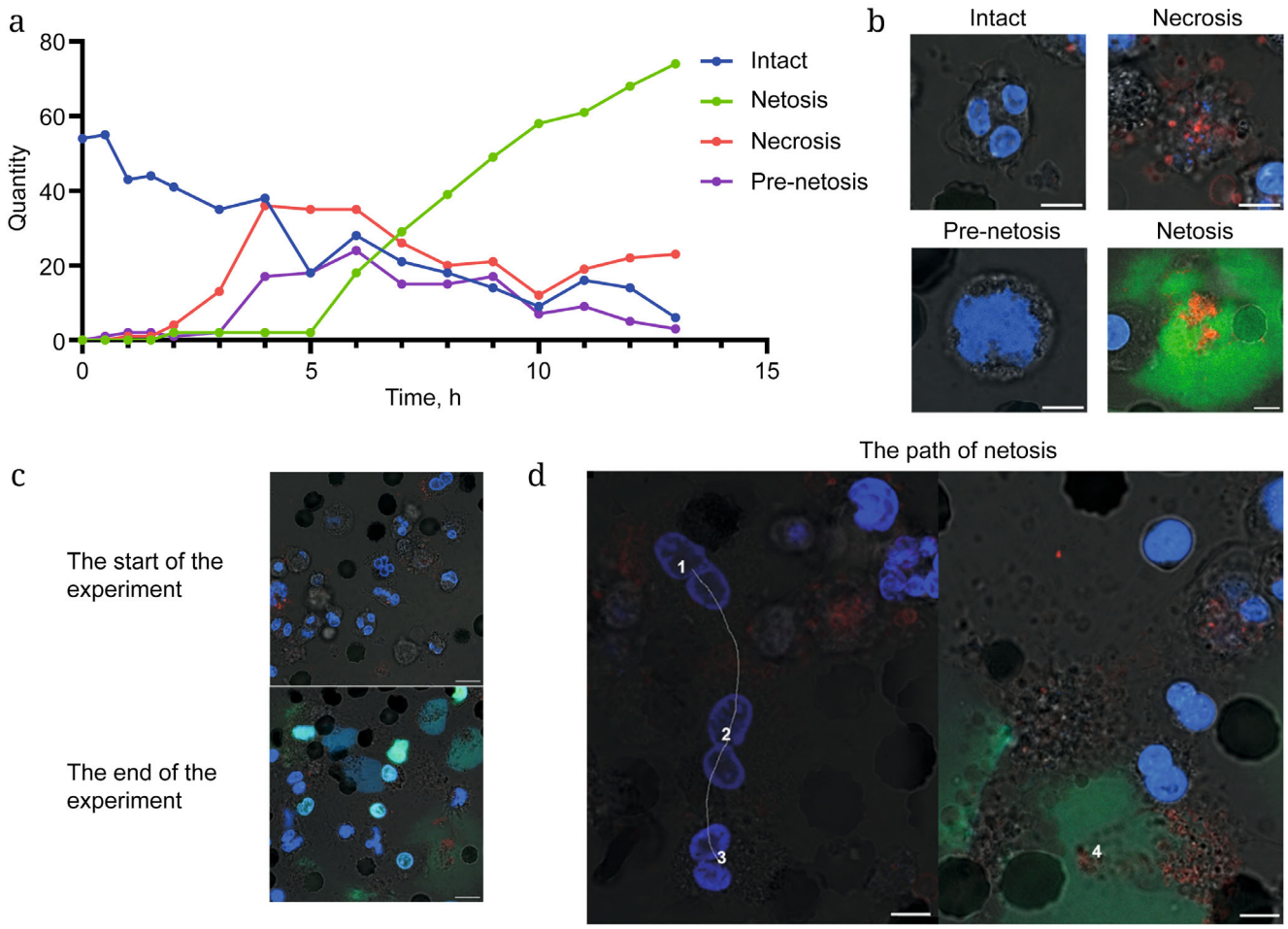

Fig. 4. Scenarios of regulated neutrophil death in response to PMA stimulation in the flow chamber. a) Dynamics of neutrophil states during the experiment. At each time point, cells of each group were counted in 16 fields of view. Number of cells in a field of view could vary because of neutrophil movement. b) Typical images of neutrophils in the state of necrosis and NETosis. Blue – Hoechst 33342 (DNA); green – Sytox Green (extracellular DNA); red – annexin V-AF647 (phosphatidylserine). Scale bar: 5 μm. c) General view of a typical field of view and leukocyte states. Scale bar: 10 μm. d) Typical movement of a neutrophil before NETosis. The figure shows trajectory of a cell, its final position, and its outcome (NETosis) at the end of the experiment. Time points: 1) 0 h, 2) 1.5 h, 3) 3.5 h, 4) 8 h. Scale bar: 10 μm.

neutrophils (which in this work are consistent with the previous data [15]). This important effect could be related to the neutrophil activation during isolation, to the influence of the substrate used for the cell immobilization in microscopy, or to the antioxidant properties of blood plasma. These results raise the question of optimal conditions for the NETosis studying.

The findings are of primary interest for refining further research into NETosis, as well as for standardizing and increasing reproducibility of the clinical laboratory methods related to the detection of ROS, NETosis, and neutrophil degranulation. From a fundamental standpoint, the obtained data provide a basic time course of the hierarchy for the development of different neutrophil activation processes as a function of activator concentration; from a methodological standpoint, they highlight strong dependence of the experimental outcomes on the environment and importance of distinguishing between the various scenarios of neutrophil lytic death.

Abbreviations

LRP	leukocyte-rich plasma
PMA	phorbol 12-myristate 13-acetate
ROS	reactive oxygen species

Contributions

M. A. Panteleev – writing the text; Q. Li, A. V. Sokolov, and A. N. Sveshnikova – development of experimental protocols; E. O. Artemenko and E. A. Adamanskaya – conducting experiments, preparation of figures; M. A. Panteleev and A. N. Sveshnikova – concept and supervision of the work; all authors – discussion of the results and editing of the manuscript.

Funding
This work was financially supported by the Russian Science Foundation (grant no. 25-25-20101).

Ethics approval and consent to participate
The study was carried out in accordance with the Declaration of Helsinki and approved by the Ethics Committee of the Center for Theoretical Problems of Physicochemical Pharmacology, Russian Academy of Sciences (protocol no. 1 of January 12, 2018). Informed consent was obtained from all donors for participation in the study and publication of its results.

Conflict of interest
The authors of this work declare that they have no conflicts of interest.

REFERENCES

1. Dahlgren, C., et al. (1999) Respiratory burst in human neutrophils, *J. Immunol. Methods*, **232**, 3-14, https://doi.org/10.1016/s0022-1759(99)00146-5.
2. Bjornsdottir, H., et al. (2016) Quantification of heterotypic granule fusion in human neutrophils by imaging flow cytometry, *Data Brief*, **6**, 386-393, https://doi.org/10.1016/j.dib.2015.12.003.
3. Vorobjeva, N., et al. (2017) Mitochondrial reactive oxygen species are involved in chemoattractant-induced oxidative burst and degranulation of human neutrophils *in vitro*, *Eur. J. Cell Biol.*, **96**, 254-265, https://doi.org/10.1016/j.ejcb.2017.03.003.
4. Hoang, H. M., et al. (2021) Rac-dependent feedforward autoactivation of NOX2 leads to oxidative burst, *J. Biol. Chem.*, **297**, 100982, https://doi.org/10.1016/j.jbc.2021.100982.
5. Bjornsdottir, H., et al. (2015) Neutrophil NET formation is regulated from the inside by myeloperoxidase-processed reactive oxygen species, *Free Radic. Biol. Med.*, **89**, 1024-1035, https://doi.org/10.1016/j.freeradbiomed.2015.10.398.
6. Zhang, X., et al. (2016) Social amoebae trap and kill bacteria by casting DNA nets, *Nat. Commun.*, **7**, 10938, https://doi.org/10.1038/ncomms10938.
7. Colicchia, M., et al. (2023) Novel mechanisms of thrombo-inflammation during infection: spotlight on neutrophil extracellular trap-mediated platelet activation, *Res. Pract. Thromb. Haemost.*, **7**, 100116, https://doi.org/10.1016/j.rpth.2023.100116.
8. Lin, H., et al. (2023) NETosis promotes chronic inflammation and fibrosis in systemic lupus erythematosus and COVID-19, *Clin. Immunol.*, **254**, 109687, https://doi.org/10.1016/j.clim.2023.109687.
9. Adamanskaya, E. A., et al. (2025) NETosis and neutrophil activity quantification in pediatric patients with essential thrombocythemia, *Int. J. Mol. Sci.*, **26**, 11958, https://doi.org/10.3390/ijms262411958.
10. Vorobjeva, N., et al. (2023) Protein kinase C isoforms mediate the formation of neutrophil extracellular traps, *Int. Immunopharmacol.*, **114**, 109448, https://doi.org/10.1016/j.intimp.2022.109448.
11. Damascena, H. L., et al. (2022) Neutrophil activated by the famous and potent PMA (phorbol myristate acetate), *Cells*, **11**, 2889, https://doi.org/10.3390/cells11182889.
12. Tu, H., et al. (2024) Dying to defend: neutrophil death pathways and their implications in immunity, *Adv. Sci.*, **11**, e2306457, https://doi.org/10.1002/advs.202306457.
13. Walrand, S., et al. (2003) Flow cytometry study of polymorphonuclear neutrophil oxidative burst: a comparison of three fluorescent probes, *Clin. Chim. Acta*, **331**, 103-110, https://doi.org/10.1016/s0009-8981(03)00086-x.
14. Bass, D. A., et al. (1983) Flow cytometric studies of oxidative product formation by neutrophils: a graded response to membrane stimulation, *J. Immunol.*, **130**, 1910-1917.
15. Patel, A. K., et al. (1987) Threshold responses in production of reactive oxygen metabolites in individual neutrophils detected by flow cytometry and microfluorimetry, *Biochem. J.*, **248**, 173-180, https://doi.org/10.1042/bj2480173.

Publisher's Note. Pleiades Publishing remains neutral with regard to jurisdictional claims in published maps and institutional affiliations. AI tools may have been used in the translation or editing of this article.